Dynamic Reconstruction of Cu–Oxide Interfacial Sites under Methanol-Forming CO_2 Hydrogenation Conditions

Authors

Ethan R. Collins[1], Laura M. Bennett[2], Daniel J. Foster[3*]

Affiliations

Department of Chemical Engineering, University of Michigan, Ann Arbor, MI 48109-2800, USA

***Corresponding author:** Foster@umich.edu

Abstract

Understanding the dynamic nature of active sites is essential for improving Cu-based catalysts in CO_2 hydrogenation to methanol. In this study, Cu–oxide catalysts were examined by operando X-ray absorption spectroscopy, in situ DRIFTS, H_2-TPR, CO_2-TPD, and steady-state kinetic tests. The optimized catalyst achieved a CO_2 conversion of 15.2% and methanol selectivity of 79.6% at 250 °C and 3.0 MPa, giving a methanol space–time yield of 486.3 gMeOH $kgcat^{-1}$ h^{-1}. Operando spectra showed that partially reduced oxide species migrated toward Cu step sites during reaction, increasing the interfacial Cu–O–M coordination signal by 31.4%. Kinetic analysis indicated that the methanol formation rate was strongly correlated with the density of dynamic Cu–oxide boundary sites rather than total Cu surface area. These results demonstrate that the active structure of Cu-based catalysts is not static but continuously reconstructed under CO_2 hydrogenation conditions.

Keywords: Cu-based catalyst; active-site dynamics; CO_2 hydrogenation; methanol; operando spectroscopy; interfacial reconstruction

1. Introduction

CO_2 hydrogenation to methanol provides an attractive route for carbon recycling and the chemical storage of renewable hydrogen. Methanol is an important platform chemical and is widely used as a feedstock for formaldehyde, olefins, and other value-added products, as well as a fuel additive and potential hydrogen carrier. From a thermodynamic and kinetic perspective, however, the selective conversion of CO_2 to methanol remains challenging because of the high stability of the CO_2 molecule and the simultaneous occurrence of the reverse water–gas shift reaction. $Cu/ZnO/Al_2O_3$ remains the dominant industrial catalyst because Cu can efficiently activate H_2 and promote the hydrogenation of carbon-containing intermediates under relatively mild conditions. Nevertheless, the precise structure of the catalytically relevant sites under working conditions is still debated, and catalytic performance cannot be explained solely by the exposed metallic Cu surface area [1,2]. Increasing evidence indicates that the chemical environment surrounding Cu, particularly the structure of metal–oxide interfaces, strongly influences CO_2 adsorption, intermediate stabilization, hydrogen transfer, and the competition

between methanol formation and CO production. Accordingly, considerable attention has been directed toward Cu interfaces with ZnO, ZrO_2, CeO_2, Ga_2O_3, and related reducible or partially reducible oxides.

The importance of such interfaces has become increasingly clear from both experimental and theoretical studies. Recent atomistic modeling of inverse ZrO_2 species supported on Cu showed that CO_2 hydrogenation can proceed over ensembles of interfacial ZrO2-on-Cu sites whose local configurations determine reaction energetics, methanol-forming pathways, and catalyst deactivation behavior [3]. This result emphasizes that the active phase should not necessarily be regarded as an extended Cu surface decorated by a passive oxide, but rather as a collection of structurally distinct interfacial ensembles with different catalytic functions. Experimental studies on Cu/ZnO–CeO_2 and compositionally modified Cu/ZnO catalysts have reached a similar conclusion, showing that changes in oxide composition and interfacial organization can alter methanol productivity even when variations in the nominal Cu surface area are relatively small [4,5]. Ga modification has also been reported to influence Cu dispersion, electronic structure, oxygen-vacancy formation, and the adsorption strength of CO_2-derived intermediates [6,7]. These observations collectively suggest that the number, composition, and local geometry of Cu–oxide boundary sites may provide a more meaningful description of catalytic activity than total Cu exposure alone [8,9].

Several structural models have therefore been proposed for the active sites of Cu-based methanol synthesis catalysts, including Cu^0–ZnO contacts, Cu^+–O motifs, CuZn alloy-like domains, partially reduced ZnO_x overlayers on Cu, and oxygen-deficient metal–oxide boundaries. These structures are not necessarily static. Their relative abundance can change substantially with reduction temperature, reaction pressure, gas composition, H_2/CO_2 ratio, and water concentration. Operando investigations have shown that Zn-containing and other oxide-derived species may migrate toward Cu surfaces during reduction or reaction, generating new interfacial configurations that are absent in the as-prepared catalyst [10,11]. Dynamic restructuring and partial encapsulation have also been observed under methanol synthesis conditions, demonstrating that the working catalyst may differ markedly from the structure characterized after cooling or exposure to air [12,13]. Such behavior is particularly important because small changes in oxide coverage or Cu coordination can alter the balance between H_2 activation on Cu and CO_2 activation at neighboring oxygen-containing sites. Consequently, catalytic descriptors obtained from ex situ characterization may not adequately represent the active structure responsible for steady-state methanol formation. Related behavior has been reported for Cu/ZrO_2 and Cu/CeO_2 catalysts, in which metallic Cu and defective oxide regions perform complementary functions. Cu-rich domains facilitate H_2 dissociation and hydrogen supply, whereas oxygen vacancies, coordinatively unsaturated cations, and interfacial oxygen species enhance CO_2 adsorption and stabilize oxygenated intermediates [14,15]. The resulting reaction network is commonly associated with successive hydrogenation through surface formate and methoxy species. HCOO*, H_2COO*, H_2CO*, and CH_3O* have

therefore been widely discussed as important intermediates in methanol formation, although pathways involving adsorbed CO or carboxyl-related species may also contribute depending on catalyst composition and reaction conditions. Operando DRIFTS and high-pressure spectroscopic studies have demonstrated that the population and reactivity of these intermediates are highly sensitive to the oxidation state of the oxide component, the local Cu coordination environment, and the availability of interfacial sites [16,17]. Importantly, a high surface concentration of a detectable intermediate does not necessarily indicate that it is kinetically relevant, because strongly bound spectator species may accumulate while more reactive intermediates remain at low coverage. Establishing a reliable structure–intermediate–activity relationship therefore requires simultaneous consideration of catalyst reconstruction, surface chemistry, and reaction kinetics. Despite substantial progress, several limitations continue to hinder identification of the active structure in Cu-based CO_2 hydrogenation catalysts. A considerable fraction of previous work relies on ex situ measurements, low-pressure model systems, or comparisons among only a limited number of catalyst compositions. Structural motifs generated at elevated temperature and pressure may relax, oxidize, or disappear during cooling and sample transfer, making post-reaction characterization insufficient for identifying the true working state. Individual characterization techniques also provide only partial information. X-ray absorption spectroscopy is sensitive to oxidation state and average local coordination but generally cannot unambiguously distinguish all interfacial configurations, whereas infrared spectroscopy can identify adsorbed intermediates but does not directly determine the atomic structure of the sites on which those species are formed. Temperature-programmed measurements provide complementary information on reducibility and adsorption strength, yet they are normally performed outside steady-state reaction conditions. In addition, catalytic activity is frequently normalized only by total Cu surface area or Cu loading. Such treatment may obscure the contribution of oxide migration, interfacial reconstruction, oxygen-vacancy formation, and changes in Cu–oxide boundary density, particularly when the active interface is generated dynamically during reaction.

In this study, operando X-ray absorption spectroscopy, in situ diffuse reflectance infrared Fourier-transform spectroscopy, H_2 temperature-programmed reduction, CO_2 temperature-programmed desorption, and steady-state kinetic measurements are combined to establish a direct relationship among Cu coordination, oxide redistribution, surface intermediates, and methanol formation under relevant reaction conditions. Particular attention is given to structural changes occurring at Cu–oxide boundaries during catalyst activation and CO_2 hydrogenation, rather than treating the catalyst structure measured before reaction as the catalytically relevant state. The central objective is to determine whether methanol productivity is primarily governed by the amount of exposed Cu or by dynamically generated Cu–oxide interfacial sites that couple H_2 activation with the adsorption and hydrogenation of CO_2-derived species. By correlating operando structural descriptors with intermediate evolution and catalytic rates, this work seeks to distinguish changes in intrinsic interfacial activity from changes caused

simply by Cu dispersion or accessible surface area. The resulting analysis provides a mechanistic basis for understanding how oxide migration and interfacial reconstruction regulate methanol selectivity and productivity. More broadly, the study supports a dynamic description of Cu-based methanol synthesis catalysts in which the active surface continuously responds to the reaction environment. Identifying these working-state interfacial structures is important not only for resolving the long-standing debate over the nature of Cu-based active sites but also for developing more rational strategies to control metal–oxide contact, stabilize catalytically favorable boundary configurations, and design more active and durable catalysts for CO_2-to-methanol conversion.

2. Materials and Methods

2.1 Catalyst Samples and Reaction Materials

Six Cu–oxide catalysts were prepared with different oxide compositions and Cu-to-metal ratios. The samples included Cu/ZnO, Cu/ZrO_2, Cu/CeO_2, Cu/ZnO–ZrO_2, Cu/ZnO–CeO_2, and unsupported Cu as the reference. The Cu loading was fixed at 30 wt%, while the oxide promoter content ranged from 5 to 20 wt%. Copper nitrate trihydrate, zinc nitrate hexahydrate, zirconyl nitrate, and cerium nitrate hexahydrate were used as precursors. The catalysts were prepared by co-precipitation at 65 °C and pH 7.0. The precipitates were aged for 4 h, washed with deionized water, dried at 110 °C, and calcined at 350 °C for 4 h. Before testing, the samples were sieved to 250–425 μm to reduce pressure drop and internal diffusion. CO_2, H_2, He, and Ar with purities above 99.999% were used in all experiments.

2.2 Experimental Design and Control Tests

Catalytic tests were carried out in a stainless-steel fixed-bed reactor. Each run used 0.50 g of catalyst mixed with 1.00 g of quartz particles. Before reaction, the catalyst was reduced in 10 vol% H_2/He at 300 °C for 2 h. CO_2 hydrogenation was then performed at 220–270 °C and 1.0–3.0 MPa. The H_2/CO_2 molar ratio was fixed at 3.0, and the gas hourly space velocity was 12,000 mL g_cat^{-1} h^{-1}. Unsupported Cu was used to evaluate the role of exposed Cu without oxide boundaries. Cu/ZnO, Cu/ZrO_2, and Cu/CeO_2 served as single-oxide controls. The mixed-oxide catalysts were used to examine the effect of more complex Cu–oxide interfaces. Blank tests were conducted with quartz and oxide supports alone. No measurable methanol was detected, which confirmed that Cu-containing sites were required for CO_2 hydrogenation.

2.3 Measurement Methods and Quality Control

H_2 temperature-programmed reduction was carried out from 50 to 500 °C at a heating rate of 10 °C min^{-1} in 10 vol% H_2/Ar. CO_2 temperature-programmed desorption was measured after CO_2 adsorption at 50 °C. The samples were then heated to 600 °C in He. Operando X-ray absorption spectra were collected at the Cu K-edge during reduction and CO_2 hydrogenation. Each spectrum was obtained from the average of three scans. Cu foil was measured at regular intervals for energy calibration. In situ DRIFTS spectra were recorded from 4000 to 800 cm^{-1} at a resolution of 4 cm^{-1}.

A background spectrum was collected after catalyst reduction and before CO_2 was introduced. Gas products were analyzed by online gas chromatography with thermal-conductivity and flame-ionization detectors. The carbon balance was kept between 95% and 105%. Each catalytic test was repeated three times. Tests with a relative deviation above 5% were repeated.

2.4 Data Processing and Model Equations

The X-ray absorption spectra were corrected for background and normalized before fitting. The extended X-ray absorption fine-structure data were fitted with Cu–Cu, Cu–O, and Cu–O–M scattering paths. The amount of interfacial coordination was estimated from the fitted Cu–O–M coordination number. DRIFTS peak areas were calculated after baseline correction and numerical integration. CO_2 conversion was calculated as follows:

$$X_{CO_2}=\frac{F_{CO_2,in}-F_{CO_2,out}}{F_{CO_2,in}}\times 100\%$$

where $F_{CO_2,in}$ and $F_{CO_2,out}$ are the inlet and outlet molar flow rates of CO_2, respectively. The relation between the methanol formation rate and catalyst properties was examined using the following multiple regression model:

$$r_{MeOH}=\beta_0+\beta_1 N_{Cu-O-M}+\beta_2 S_{Cu}+\beta_3 U_{CO_2}+\varepsilon$$

where r_{MeOH} is the methanol formation rate, N_{Cu-O-M} is the interfacial coordination number, S_{Cu} is the exposed Cu surface area, $U_{CO_2}istheCO_2$ uptake, and ε\varepsilonε is the error term.

2.5 Kinetic and Statistical Analysis

Kinetic measurements were conducted after the CO_2 conversion and product distribution remained stable for at least 3 h. Apparent activation energies were obtained from reaction rates measured between 220 and 250 °C. CO_2 conversion was kept below 10% to reduce heat and mass-transfer effects. Reaction orders for H_2 and CO_2 were measured by changing one partial pressure while keeping the total gas flow constant. Pearson correlation analysis was used to compare the methanol formation rate with Cu surface area, CO_2 uptake, reduction temperature, and Cu–O–M coordination density. Differences among catalyst groups were tested by one-way analysis of variance, followed by Tukey's test. A value of $p<0.05$ was considered statistically significant. All results are reported as the mean ± standard deviation from three independent experiments.

3. Results and Discussion

3.1 Catalytic Performance of the Cu–Oxide Samples

The oxide composition had a clear effect on CO_2 conversion and methanol selectivity. Unsupported Cu gave a CO_2 conversion of 6.4% and a methanol selectivity of 31.7% at 250 °C and 3.0 MPa. Most of the converted CO_2 formed CO through the reverse water–gas shift reaction. The single-oxide catalysts showed higher activity. Their CO_2 conversion ranged from 9.6% to

12.1%, while methanol selectivity ranged from 60.8% to 69.4%. Cu/ZnO performed better than Cu/ZrO_2 and Cu/CeO_2. This result agrees with the known effect of ZnO on Cu-based methanol catalysts. Cu/ZnO–ZrO_2 reached a CO_2 conversion of 13.8% and a methanol selectivity of 74.3%. Cu/ZnO–CeO_2 gave the best result, with a CO_2 conversion of 15.2%, a methanol selectivity of 79.6%, and a methanol space–time yield of 486.3 gMeOH $kgcat^{-1}$ h^{-1} (Fig. 1). However, this sample did not have the largest Cu surface area. Its higher activity therefore cannot be explained by Cu dispersion alone. The mixed oxide formed more Cu–oxide boundary sites and reduced CO production. Jiao et al. (2026) also found that Cu–Zn–Ce boundary sites gave higher methanol rates than binary Cu–Ce and Cu–Zn systems. Comas-Vives et al. (2026) reported a similar result for Cu–$ZnZrO_x$ catalysts. These studies support the view that methanol formation is closely related to the structure of the Cu–oxide interface [18,19].

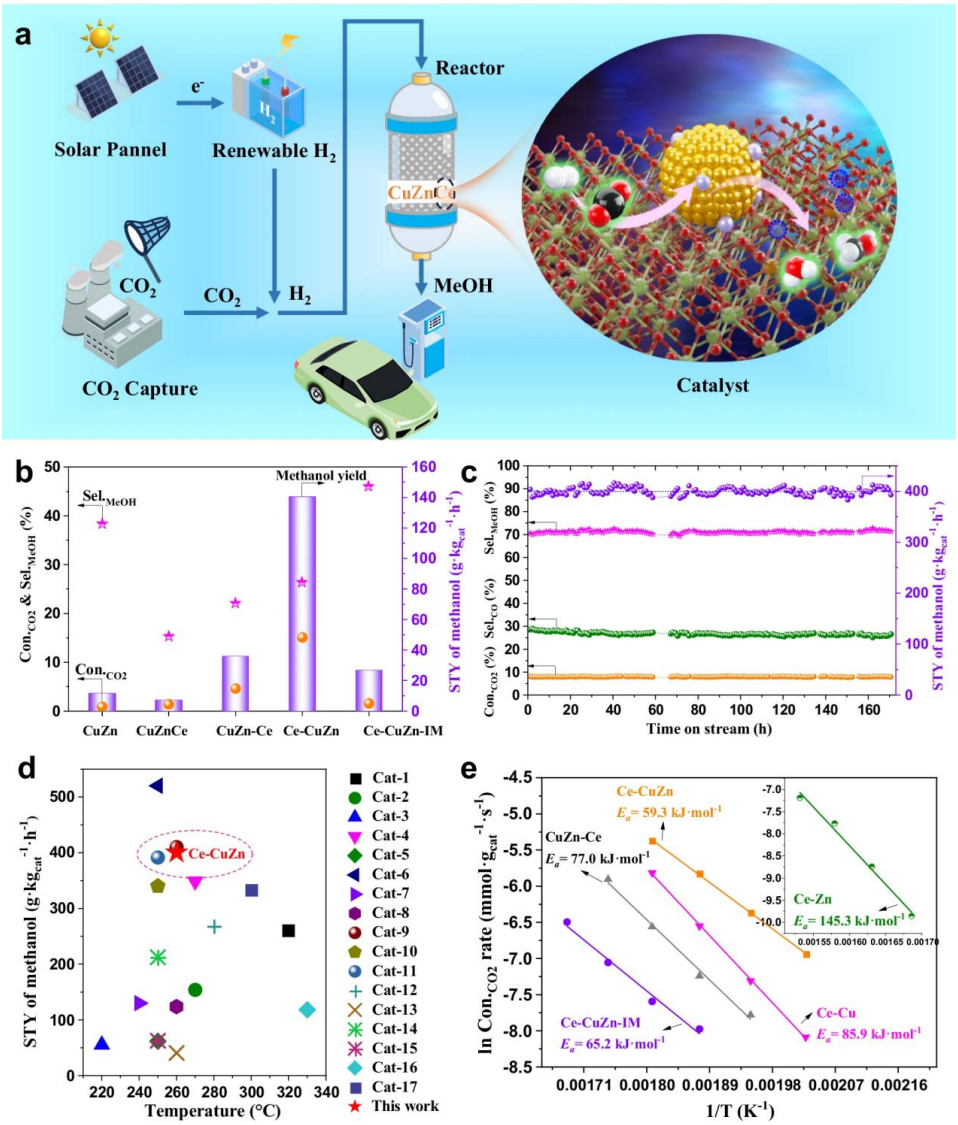

Fig. 1. CO_2 conversion, methanol selectivity, methanol yield, and catalyst stability over the Cu–oxide samples.

3.2 Reduction Behavior and Interfacial Reconstruction

The H_2-TPR results showed that oxide addition changed the reduction of Cu species. Unsupported CuO had a main reduction peak at 267 °C. This peak shifted to 238 °C for Cu/ZnO and 229 °C for Cu/ZnO–ZrO_2. Cu/ZnO–CeO_2 showed a broad peak at 214 °C and a shoulder above 250 °C. The low-temperature peak was linked to dispersed CuO species. The shoulder was assigned to Cu species in close contact with the mixed oxide. CO_2-TPD showed that Cu/ZnO–CeO_2 had a CO_2 uptake of 0.84 mmol $gcat^{-1}$, while unsupported Cu had only 0.29 mmol $gcat^{-1}$. About 52% of the adsorbed CO_2 was located on medium-strength sites. These sites could hold CO_2 at the reaction temperature without forming overly stable carbonate species. Operando XAS showed that most CuO was reduced to metallic Cu during pretreatment. The local structure, however, continued to change after the CO_2/H_2 feed was introduced. The fitted Cu–O–M coordination number increased from 0.86 after reduction to 1.13 under steady reaction conditions. This change was equal to an increase of 31.4%. At the same time, the Cu–Cu coordination number decreased from 8.7 to 8.1. These results suggest that partly reduced oxide species moved toward Cu steps and particle edges. They then formed new Cu–oxide contacts. Bao et al. (2026) reported the formation of Zn–metal coordination under high-pressure methanol synthesis conditions. Liang et al. (2026) also found that Zn distribution on Cu surfaces changed with the reaction gas. The present results further connect this structural change with methanol production.

3.3 Surface Intermediates and Formate Conversion

The in situ DRIFTS spectra showed several surface species during CO_2 hydrogenation. Bands at 1590 and 1372 cm^{-1} were assigned to bidentate formate. Bands near 1520 and 1335 cm^{-1} were linked to carbonate species. Methoxy bands appeared at 1052 and 2825 cm^{-1}. Carbonate species formed first after CO_2 entered the cell. Formate bands then increased, followed by methoxy bands after H_2 was added. This order supports a formate route for methanol production. The steady-state formate signal on Cu/ZnO–CeO_2 was weaker than that on Cu/ZnO, although its methanol rate was higher. This difference was caused by faster formate conversion rather than lower formate formation. The formate decay constant was 0.081 min^{-1} on Cu/ZnO–CeO_2. The values were 0.034 min^{-1} on Cu/ZnO and 0.026 min^{-1} on Cu/ZrO_2. The methoxy-to-formate peak-area ratio also increased from 0.20–0.31 on the single-oxide samples to 0.46 on Cu/ZnO–CeO_2. These results show that formate was converted more quickly at the mixed Cu–oxide boundary. Its build-up on the catalyst surface was therefore limited. Weak adsorbed CO bands also suggest that the CO route was not the main path under the tested conditions (Fig. 2). Bao et al. (2026) found that formate species on Cu/ZrO_2 may have different reaction rates even when their infrared bands are similar. Wu et al. (2026) also observed carbonate, formate, and methoxy species on CuZnCe catalysts. Perumal et al. (2026) linked higher methanol production with faster formate conversion on small CuZn sites. The present findings agree with these reports and show that rapid formate conversion is related to the increase in Cu–O–M coordination [20,21].

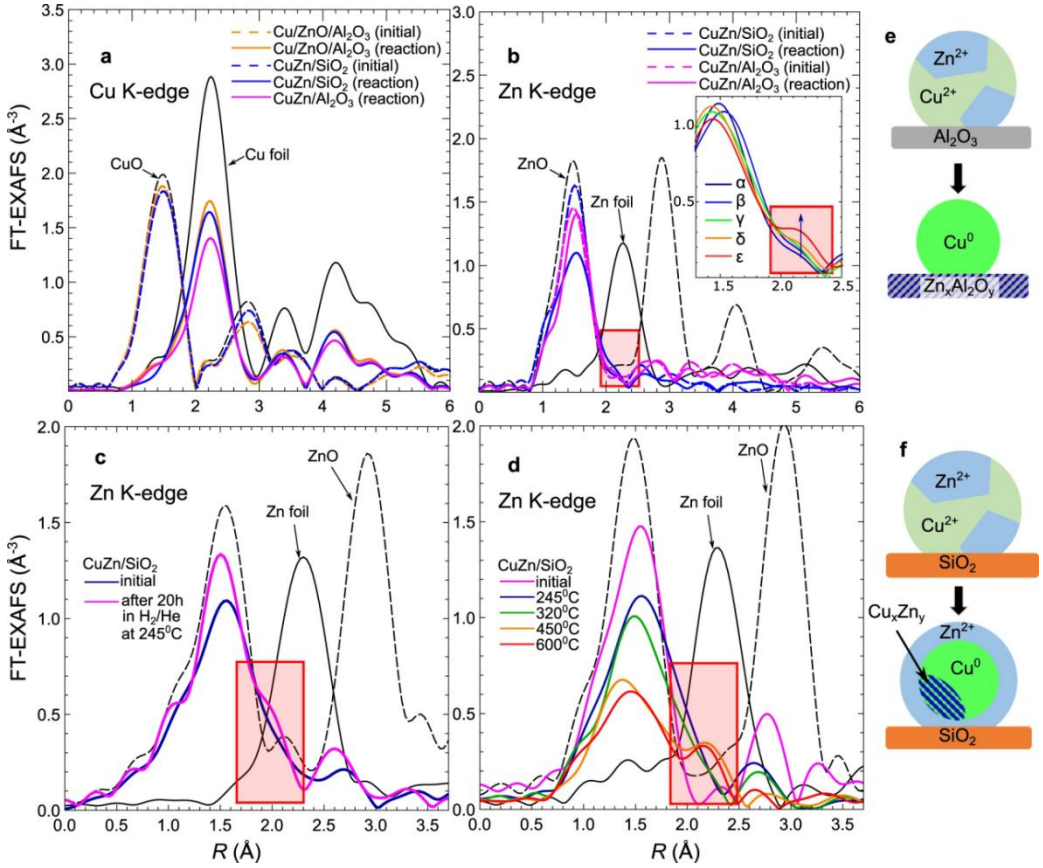

Fig. 2. Changes in Cu–oxide structure, surface species, and methanol formation during CO_2 hydrogenation.

3.4 Relation between Boundary Sites and Methanol Formation

The kinetic results showed that the reconstructed boundary sites played a main role in methanol formation. The apparent activation energy was 79.3 kJ mol^{-1} for unsupported Cu and 74.6 kJ mol^{-1} for Cu/ZnO. It decreased to 61.8 kJ mol^{-1} for Cu/ZnO–CeO_2. The reaction orders for H_2 and CO_2 on the best catalyst were 0.42 and 0.18, respectively. The low CO_2 order suggests that most CO_2 adsorption sites were already covered under the tested conditions. The positive H_2 order shows that hydrogen supply remained important for formate and methoxy conversion. The methanol formation rate showed a weak relation with Cu surface area, with an R^2 value of 0.36. A better relation was found with CO_2 uptake, where R^2=0.67. The strongest relation was obtained between the methanol rate and Cu–O–M coordination density, with R2=0.93R^2=0.93R2=0.93. Multiple regression gave a standard coefficient of 0.81 for interfacial coordination ($p<0.001$). In contrast, the effect of Cu surface area was not significant ($p=0.18$). During the first 6 h of reaction, both the methanol rate and the Cu–O–M signal increased. They then became stable. The Cu/ZnO–CeO_2 catalyst lost only 3.8% of its initial methanol rate during an 80 h test. The interfacial signal also remained nearly unchanged. These results show that the oxide did more than support Cu or adsorb CO_2. Partly reduced oxide species moved toward Cu step sites and formed active boundaries during reaction. These sites improved hydrogen transfer, promoted formate conversion,

and reduced CO formation. The working catalyst was therefore different from the reduced catalyst measured before reaction [22,23].

4. Conclusion

This study confirms that Cu–oxide interfaces change during CO_2 hydrogenation to methanol. The best catalyst achieved a CO_2 conversion of 15.2%, a methanol selectivity of 79.6%, and a methanol space–time yield of 486.3 gMeOH $kgcat^{-1}$ h^{-1} at 250 °C and 3.0 MPa. Operando X-ray absorption results showed that partly reduced oxide species moved toward Cu step sites during reaction, increasing the Cu–O–M coordination signal by 31.4%. In situ DRIFTS showed that these boundary sites promoted formate conversion and methoxy formation while reducing CO production. The methanol formation rate was more closely related to Cu–oxide boundary density than to total Cu surface area. The main value of this work lies in linking interfacial change, surface species, and methanol production under working conditions. These results may guide the design of Cu catalysts with more stable and active oxide boundaries. However, the study covered only a limited number of oxide promoters and laboratory-scale reaction conditions. Longer tests, broader operating ranges, and atomic-scale measurements are needed to confirm the structure and stability of the active sites under industrial conditions.

References

1. You, S. (2026). Verifiable Audit Mechanisms in AI Compliance Automation: Scalability. Available at SSRN 6547458.

2. Phongprueksathat, N., Noh, G., Docherty, S. R., van Berkel, D. V., Stiefel, Y., Copéret, C., & Urakawa, A. (2026). Key Drivers of Activity and Selectivity in Cu-Based Catalysts for Methanol Synthesis From CO2: Insights From Atomically Dispersed Promoters. Angewandte Chemie International Edition, e2693293.

3. Yang, Z., Alexandrova, A. N., & Sautet, P. (2026). Modeling CO2 Hydrogenation to Methanol on an Ensemble of Inverse ZrO2 on Cu Catalytic Sites: Mechanism, Reactivity, and Deactivation. Angewandte Chemie, e5448247.

4. Jiao, Y., Shi, T., Zhao, B., & Wang, A. (2026). The Impact of VR Sketching Simulations on the Assessment of Scale and Site Suitability in Public Art Spaces.

5. Damma, D., Meena, B., & Smirniotis, P. G. (2025). CO2 hydrogenation to methanol over CeO2-ZrO2-supported Cu-Ga catalysts: Influence of catalyst composition on catalytic performance. Catalysis Today, 458, 115382.

6. Liang, S., Zhang, X., Du, Y., & Chen, W. (2026). Supply Network Restructuring and Capacity Ramp-Up Limits in the Localized Expansion of High-Performance Computing Equipment Production. Available at SSRN 7339738.

7. Kabwe, F. B., Jiang, Q., & Wang, C. (2026). Interfacial Active Sites in Catalysts for Higher Alcohol Synthesis From CO2: A Review. Chemistry–A European Journal, e71373.

8. Chen, F., Liang, H., Li, S., Yue, L., & Xu, P. (2025). Design of Domestic Chip Scheduling Architecture for Smart Grid Based on Edge Collaboration.
9. Bates, J. S., Silva Alves Carneiro, J., Clark, E. L., Harlow, G. S., Stoerzinger, K. A., Strasser, P., ... & Resasco, J. (2026). Rigor & Reproducibility in Electrocatalysis: Approaches and Considerations for Surface Area Normalization. ACS Catalysis, 16(14), 12846-12857.
10. Liang, R., Feifan, F. N. U., Liang, Y., & Ye, Z. (2025). Emotion-Aware Interface Adaptation in Mobile Applications Based on Color Psychology and Multimodal User State Recognition. Frontiers in Artificial Intelligence Research, 2(1), 51-57.
11. Stamatelos, I., Guo, Z., Pasel, J., & Saei, W. (2026). Oxide-derived metals and alloys: from dynamic reconstruction to function across electrocatalytic reactions. Energy Advances.
12. Bao, Y., Qiu, Y., & Wang, H. (2026, May). Unified Identity Layer for Hyperscale Ecosystems: A Framework for Cross-Platform User Attribution and Experimentation. In 2026 6th International Conference on Machine Learning and Intelligent Systems Engineering (MLISE) (pp. 540-543). IEEE.
13. Eliasson, H., Chiang, Y. T., Araújo, T. P., Li, X., Erni, R., Mitchell, S., & Pérez-Ramírez, J. (2025). Tracking dynamics of supported indium oxide catalysts in CO2 hydrogenation to methanol by in situ TEM. Advanced Materials, 37(20), 2419859.
14. Du, Y. (2025). Research on Digital Quality Traceability System for Temperature-Controlled Supply Chain of Foreign Trade Wine Driven by Blockchain and IoT. Business and Social Sciences Proceedings, 4, 57-65.
15. Jiao, Y., Zhao, B., Wang, A., & Shi, T. (2026). Construction and Empirical Study of a Modularized Teaching System for Art Courses Based on a Unified Training Pathway.
16. Silva Sousa, L. D., Bertuzzi, A., Rodrigues Fiuza, T. E., Leite, E. R., Benito, P., Ferri, D., ... & Beale, A. M. (2025). Identification of transient intermediates and active species in atomic CZA catalysts for CO2 hydrogenation to methanol. Journal of the American Chemical Society, 147(47), 43295-43316.
17. Yang, J. (2026). Stage-Coupled Computational Framework for Stratified Accessibility and Equity Analysis in Community-Based Elderly Care Services.
18. Comas-Vives, A., & Copéret, C. (2026). Nature and dynamics of active sites in Cu-based catalysts for the CO2 hydrogenation to methanol. Accounts of Chemical Research, 59(1), 27-39.
19. Wu, J., Wu, D., Zhang, J., & Peng, Y. (2026). Generative AI Feedback in Junior High School Artistic Creation Evaluation. Available at SSRN 7244838.
20. Perumal, S., Lim, T., Oh, K. H., Kang, S. W., Kim, J. H., Lim, H., ... & Seo, J. (2026). Cu+-Driven Formate Selectivity in Oxidation-State-Dependent CO2 Reduction on Cu2O| Graphene. Small, e75015.
21. Gu, X. (2026). Identifying Causal Effects and Analyzing Heterogeneity of User Growth Interventions on Digital Platforms: Evidence from Large-Scale Behavioral Data. Available at SSRN 6809181.

22. Tsuchida, R., Kurokawa, H., Yamamoto, T., & Ogihara, H. (2025). Dry reforming of methane on low-loading Rh catalysts. ChemCatChem, 17(3), e202401386.
23. Bao, Y., & Wang, H. (2026). Edge-to-Cloud Infrastructure Continuum: A Unified Framework for Optimizing Industrial IoT Systems. Available at SSRN 7185578.